

## Modulational instability of Gross-Pitaevskii-type equations in 1+1 dimensions

G. Theocharis,<sup>1</sup> Z. Rapti,<sup>2</sup> P. G. Kevrekidis,<sup>2</sup> D. J. Frantzeskakis,<sup>1</sup> and V. V. Konotop<sup>3</sup>

<sup>1</sup>*Department of Physics, University of Athens, Panepistimiopolis, Zografos, Athens 15784, Greece*

<sup>2</sup>*Department of Mathematics and Statistics, University of Massachusetts, Amherst, Massachusetts 01003-4515, USA*

<sup>3</sup>*Centro de Física Teórica e Computacional, Universidade de Lisboa, Avenida Professor Gama Pinto, 2, Lisboa 1649-003, Portugal*

(Received 27 December 2002; published 26 June 2003)

The modulational instability of the nonlinear Schrödinger (NLS) equation is examined in the case with a quadratic external potential. This study is motivated by recent experimental results in the context of matter waves in Bose-Einstein condensates (BECs). The theoretical analysis invokes a lens-type transformation that converts the Gross-Pitaevskii into a modified NLS equation without explicit spatial dependence. This analysis suggests the particular interest of a specific time-varying potential [ $\sim(t+t^*)^{-2}$ ]. We examine both this potential, as well as the time-independent one numerically and conclude by suggesting experiments for the production of solitonic wave trains in BECs.

DOI: 10.1103/PhysRevA.67.063610

PACS number(s): 03.75.Kk, 03.75.Lm, 42.65.Sf

### I. INTRODUCTION

Intensive studies of Bose-Einstein condensates (BECs) [1] have drawn much attention to nonlinear excitations in them. Recent experiments have achieved to generate topological structures, such as vortices [2] and vortex lattices [3], as well as solitons. Especially, as far as the latter are concerned, two types of solitons have been created, namely, *dark* solitons [4–6] for condensates with repulsive interactions and *bright* ones [7] for condensates with attractive interactions. Dark solitons are density dips characterized by a phase jump of the wave function at the position of the dip, and, thus, can be generated by means of phase-engineering techniques. Bright solitons, which were only recently created in BECs of <sup>7</sup>Li, are characterized by a localized maximum in the density profile without any phase jump across it. In the relevant experiments, this type of soliton was formed upon utilizing a Feshbach resonance to change the sign of the scattering length from positive to negative. An interesting question concerns how such solitary wave structures may arise (i.e., which is the underlying physical mechanism for their manifestation and how they may be generated) in this context of matter waves in BECs.

It is well known that the dynamics of the BEC wave function is described (at the mean-field level, which is an increasingly accurate description, as the zero-temperature limit is approached) by the Gross-Pitaevskii (GP) equation, a variant of the well-known nonlinear Schrödinger (NLS) equation [8], which incorporates an external trapping potential term. In the context of the “traditional” NLS equation (without the external potential), perhaps the most standard mechanism through which bright solitons and solitary wave structures appear is through the activation of the modulational instability (MI) of plane waves. In this case, the continuous wave (CW) solution of the NLS equation becomes unstable towards the generation of a chain of bright solitons. It is the purpose of this work to demonstrate that, under certain conditions, this may also happen in the case of the GP equation as well.

The MI is a general feature of continuum as well as of discrete nonlinear wave equations and its demonstrations

span a diverse set of disciplines, ranging from fluid dynamics [9] (where it is usually referred to as the Benjamin-Feir instability) and nonlinear optics [10] to plasma physics [11]. Additionally, the MI has been examined recently in the context of optical lattices in BECs both in one-dimensional (1D) and quasi-one-dimensional systems, as well as in multiple dimensions. In such settings, it has been predicted theoretically [12,13] and verified experimentally [14,15] to lead to destabilization of plane waves, and in turn to delocalization in momentum space (equivalent to localization in position space and the formation of solitary wave structures).

In this paper, we discuss the MI conditions for the continuous NLS equation in 1+1 dimensions (1 spatial and 1 temporal),

$$iu_t + u_{xx} + s|u|^2u + V(x)u = 0, \quad (1)$$

in the presence of the external potential  $V(x)$ . This equation is actually a dimensionless effective GP equation, which describes the evolution of the wave function of a quasi-one-dimensional cigar-shaped BEC subject to definite conditions (see below). In this context, we will consider the harmonic potential

$$V(x) = -k(t)x^2, \quad (2)$$

which is relevant, in particular, to experimental setups in which the (magnetic) trap is strongly confined in the two directions, while it is much shallower in the third one [1]. The prefactor  $k(t)$  is typically fixed in current experiments, but adiabatic changes in the strength (and, in fact, even in the location of the center) of the trap are experimentally feasible, hence we examine the more general time-dependent case.

A self-consistent reduction of a 3D GP equation to a 1D NLS equation with external potential can be provided by means of the multiple-scale expansion (see, e.g., Ref. [12] for details). In the case of a cigar-shaped BEC such an expansion exploits a small parameter  $\delta^2 = (Na_s/a_0)k \ll 1$ , where  $N$  is the number of atoms,  $a_s$  is the  $s$ -wave scattering length,  $a_0 = \sqrt{\hbar/m\omega_0}$  is the longitudinal harmonic-oscillator length,  $\omega_0$  is the harmonic frequency, and  $m$  is the atomic

mass. The parameter  $\delta$  indicates the relative strength of the two-body interactions as compared to the kinetic energy of the atoms. In the case at hand, when the finite-size effects along the cigar axes are of primary interest, the same small parameter defines strong confinement cross section and to the cigar axis by the condition  $a_{\perp}/a_0 \sim \delta\sqrt{k}$  ( $a_{\perp}$  is the transverse harmonic-oscillator length).

It is worth pointing out that, for example, for a BEC of  $N=10^4$  of  $^{23}\text{Na}$  atoms ( $a_s \approx 2.75$  nm), having characteristic sizes  $a_0=300$   $\mu\text{m}$  and  $a_{\perp}=10$   $\mu\text{m}$  one obtains  $k \approx 0.11$  and  $\delta^2 \approx 0.01$ . It should be noted that herein different values of  $k$  were used [as well as time-dependent traps where  $k=k(t)$ —see below].

In this reduction, the complex field  $u(x,t)$  in Eq. (1) represents the rescaled mean-field wave function of the condensate according to

$$\Psi(\mathbf{r},t) = \frac{\delta}{a_{\perp} a_s^{(1/2)}} e^{-i\omega_{\perp} t} e^{-r^2/(2a_{\perp}^2)} u(\delta x/a_{\perp}, \delta^2 \omega_{\perp} t/2), \quad (3)$$

where  $\Psi(\mathbf{r},t)$  is the original order parameter,  $\mathbf{r}=(y,z)$ ,  $\omega_{\perp}$  is the harmonic frequency corresponding to the cross section, and physical space and time coordinates are used. Respectively, in the reduced and rescaled GP equation (1),  $x$  is normalized to the harmonic-oscillator length  $a_{\perp}$ , time is normalized to the corresponding oscillation period, the potential  $V(x)$  is measured in units of  $\hbar^2 a_{\perp}^2/8m$ , and  $u(x,t)$  is a function of order one,  $u(x,t)=O(1)$ .

In the present paper  $a_0$  will be a varying quantity, and then in the estimates  $a_0$  should be understood as an effective averaged quantity. Notice also that in Eq. (1), the subscripts denote partial derivatives with respect to the index, while  $s = -\text{sign}(a_s) \in \{1, -1\}$  illustrates the focusing (+1) or defocusing (-1) nature of the nonlinearity (which represents the attractive or repulsive nature of the interatomic interactions, respectively [1]).

After briefly reviewing (in Sec. II) the MI for the NLS case, we proceed to our main aim that is to study this instability in the context of the GP of Eq. (1), with the potential of Eq. (2). In Sec. III, we show that a lens-type transformation, which transforms the GP equation into a relatively simpler form of the NLS equation, provides insight in the latter case. Two interesting cases are singled out: the case where  $k(t) \equiv k$  (i.e., for a fixed trap) and the case of  $k(t) \sim (t+t^*)^{-2}$ , which naturally arises in this setting. In Sec. IV, we investigate these cases numerically and find a variety of interesting results including the generation of solitary wave trains. This result indicates that the MI is indeed an underlying physical mechanism explaining the formation of matter-wave soliton trains. Finally, we conclude with the discussion of Sec. V, which suggests this method as an experimental technique for the generation of soliton patterns in BEC.

## II. MODULATIONAL INSTABILITY FOR NLS

We start by recalling the results for the modulational stability of the NLS (1) without an external potential, i.e., for  $V(x) \equiv 0$ :

$$iu_t + u_{xx} + s|u|^2 u = 0. \quad (4)$$

We look for perturbed plane-wave solutions of the form

$$u(x,t) = (\phi + \epsilon b) \exp[i\{(qx - \omega t) + \epsilon \psi(x,t)\}], \quad (5)$$

analyzing the  $O(\epsilon)$  terms as

$$b(x,t) = b_0 \exp[i\beta(x,t)], \quad \psi(x,t) = \psi_0 \exp[i\beta(x,t)]. \quad (6)$$

Using  $\beta(x,t) = Qx - \Omega t$ , the dispersion relation connecting the wave number  $Q$  and frequency  $\Omega$  of the perturbation (see, e.g., Ref. [8]) is found to be of the form

$$(-\Omega + 2qQ)^2 = Q^2(Q^2 - 2s\phi^2). \quad (7)$$

This implies that the instability region for the NLS in the absence of an external potential, appears for perturbation wave numbers  $Q^2 < 2\phi^2$ , and, in particular, *only for focusing nonlinearities* (to which we will restrict our study from this point onwards).

A natural question is how this instability is manifested for wave numbers that satisfy the above condition. An example is shown in Fig. 1.

There are two principal ways in which the instability can be detected (see Fig. 1). One of them is by probing the maxima of the original plane wave (notice that to avoid problems with the boundaries, the simulation shown in the figure was performed with periodic boundary conditions). In the modulationally unstable case, we have periodic recurrence of structures with very large amplitude, while in the modulationally stable case of  $Q=2$ , the perturbation only causes small amplitude oscillations. In the Fourier picture, the unstable perturbation generates sidebands of higher harmonics as is well known [16], while similar structures are absent in the modulationally stable case.

## III. MODULATIONAL INSTABILITY FOR NLS WITH QUADRATIC POTENTIAL

The quadratic potential of Eq. (2) is clearly the most physically relevant example of an external potential in the BEC case, given the harmonic confinement of the atoms by the experimentally used magnetic traps [1].

To examine the MI related properties in this case, we use a lens-type transformation [8] of the form

$$u(x,t) = \ell^{-1} \exp[i f(t) x^2] v(\zeta, \tau), \quad (8)$$

where  $f(t)$  is a real function of time,  $\zeta = x/\ell(t)$  and  $\tau = \tau(t)$ . To preserve the scaling, we choose [8,17]

$$\tau_t = 1/\ell^2. \quad (9)$$

The resulting equations can be satisfied by demanding that

$$f_t = -4f^2 - k(t), \quad (10)$$

$$\ell_{\tau}/\ell = 4f\ell^2. \quad (11)$$

Taking into account Eq. (9), the last equation can be solved

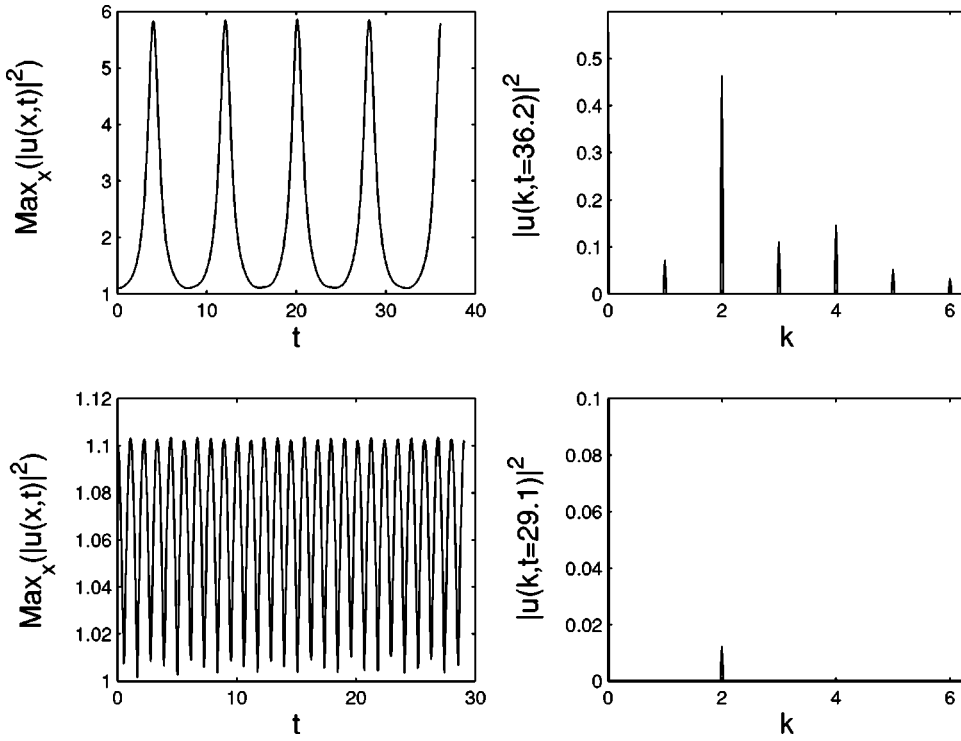


FIG. 1. The evolution of the maximum amplitude (left panels) and the Fourier transform at the ending time of the simulation (right panels), for a modulationally unstable case  $Q=1$  (top panels) and a modulationally unstable case  $Q=2$  (bottom panels). An initial perturbation of  $0.05 \sin(Qx)$  was added to the uniform solution of  $\phi=1$ .

$$\ell(t) = \ell(0) \exp\left(4 \int_0^t f(s) ds\right). \quad (12)$$

This problem of finding the time dependence of the parameters is then reduced to the solution of Eq. (10).

Upon the above conditions, the equation for  $v(\zeta, \tau)$  becomes

$$iv_\tau + v_{\zeta\zeta} + |v|^2 v - 2i\lambda v = 0, \quad (13)$$

where

$$f\ell^2 = \lambda, \quad (14)$$

and generically  $\lambda$  is real and depends on time. Thus, we retrieve NLS with an additional term, which represents either growth (if  $\lambda > 0$ ) or dissipation (if  $\lambda < 0$ ).

A particularly interesting case is that of  $\lambda$  constant. Then from the system of equations (9)–(11) and (13), it follows that  $k$  must have a specific form.  $f$ ,  $\ell$ , and  $\tau$  can then be determined accordingly. In fact, the system of equations (9)–(11) and (13) with  $\lambda$  constant has as its solution

$$k(t) = (t + t^*)^{-2}/16, \quad (15)$$

$$f(t) = (t + t^*)^{-1}/8, \quad (16)$$

$$\ell(t) = 2\sqrt{2\lambda}\sqrt{t + t^*}, \quad (17)$$

$$\tau(t) = \ln\left(\frac{t + t^*}{t^*}\right) / 8\lambda. \quad (18)$$

Notice that as per the assumption of an imaginary phase in the exponential of Eq. (8), that our considerations are valid

only for  $\lambda \in R$ . In the above equations,  $t^*$  is an arbitrary constant whose sign is related to the sign of  $\lambda$ ;  $t^*\lambda > 0$  and which essentially determines the “width” of the trap at time  $t=0$  according to Eq. (15). Notice that  $t^* < 0$  [i.e., the case of dissipation in Eq. (13)] describes a BEC in a shrinking trap, while the case  $t^* > 0$  [i.e., the case of growth in Eq. (13)] corresponds to a broadening condensate.

In this case the modulational condition remains unchanged, but now  $\omega$  satisfies the dispersion relation  $\omega = q^2 - \phi^2 + 2i\lambda$ , so the growth (if  $\lambda > 0$ ) or dissipation (if  $\lambda < 0$ ) is inherent in Eq. (5). Moreover, all the terms are modulated by the constant growth (or decay) rate  $\exp(2\lambda\tau)$ , and the instability (when present) will be developing according to the form  $v \sim \exp[i(Q\zeta - \Omega_r\tau) + (\nu + 2\lambda)\tau]$  with  $\Omega = \Omega_r + i\nu$  and  $\Omega_r = 2qQ$ .

If  $k = k(t)$  is not given by Eq. (15), then  $\lambda$  must be time dependent [e.g.,  $\lambda \equiv \lambda(t)$ ]. Here, one cannot directly perform the MI analysis. However, still in this case, we have converted the explicit spatial dependence into an explicit temporal dependence. An important example of this type (the simplest one, in fact) is the case of  $k(t) \equiv k = \text{const}$ . Then,

$$f(t) = -\frac{\sqrt{k}}{2} \tan[2\sqrt{k}(t + t^*)], \quad (19)$$

$$\ell(t) = \ell(0) \frac{\cos[2\sqrt{k}(t + t^*)]}{\cos(2\sqrt{k}t^*)}, \quad (20)$$

$$\tau(t) = -\frac{\cos^2(2\sqrt{k}t^*)}{\ell(0)^2} \frac{f(t)}{k}. \quad (21)$$

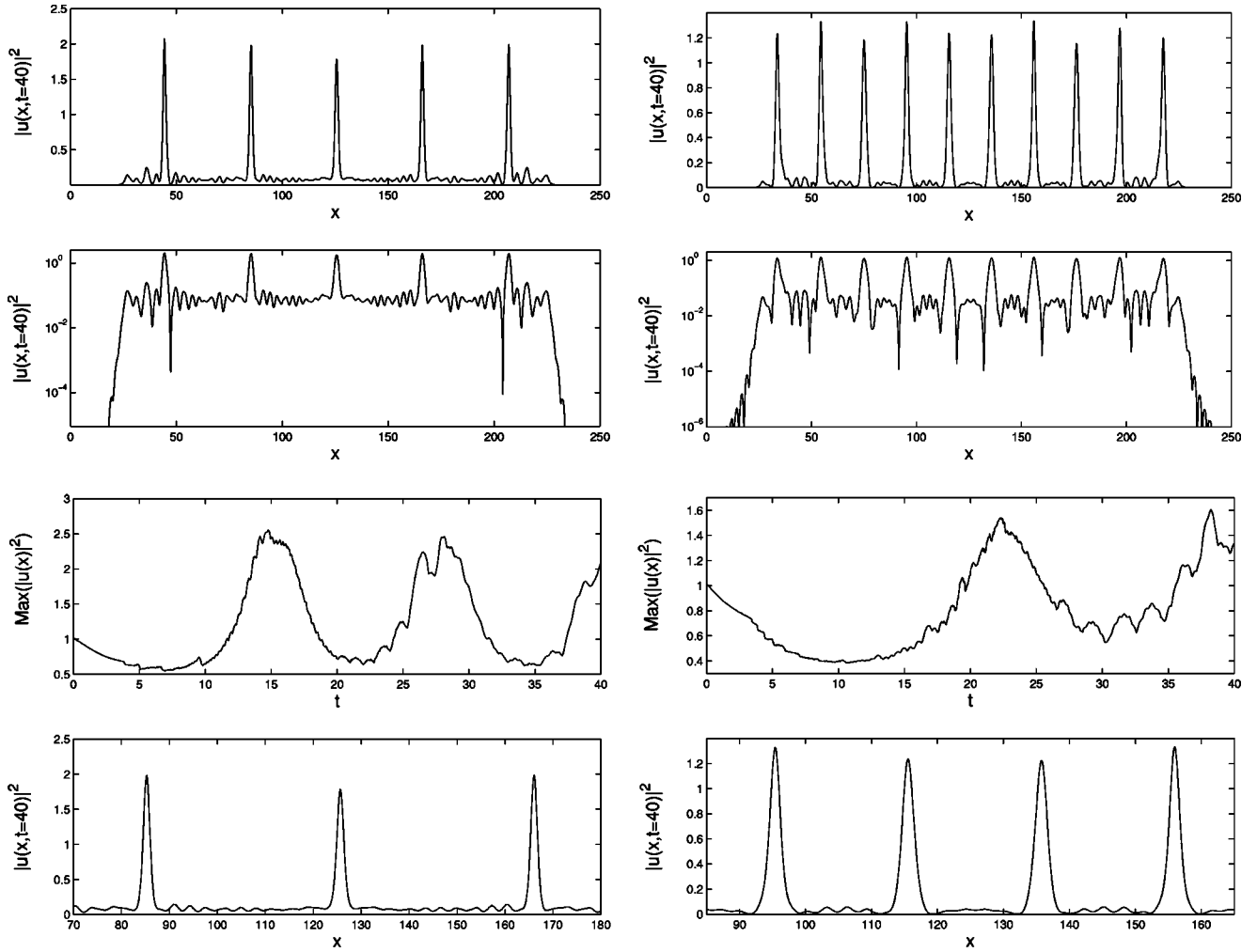


FIG. 2. The evolution of an initial condition of the form of Eq. (22) for the time-dependent potential of Eq. (15). The left panels show the case of  $Q=1$ , while the right ones the case of  $Q=2$ . The panels show, respectively: the profile of  $|u(x)|^2$  at  $t=40$ , in the top panel, the same profile is shown in a semilogarithmic plot in the second from the top panel (clearly indicating the exponential nature of the localization). The time evolution of the maximum amplitude of the configuration is shown in the third (from the top) panel, while the bottom panel shows a detail of the top one (indicating the clearly solitary structure of the corresponding pulses).

This case imposes a time-periodic driving term in Eq. (13) with frequency  $4\sqrt{k}$ , which is nothing but the oscillation frequency naturally following from the Ehrenfest theorem. In this viewpoint, the phase divergence at  $t_n = \pi(n + 1/2)/(2\sqrt{k}) - t^*$  (where  $n=0, \pm 1, \pm 2, \dots$ ) is understandable. Indeed, in the case at hand, the “chirp” initial condition means existence of a current at the initial moment of time. Due to the quadratic potential, this current periodically changes the direction (which is a straightforward consequence of the Ehrenfest theorem). The change of the current direction is accompanied by the phase singularity.

From the above it is clear that the most interesting cases in the setting with the harmonic potential are the ones with the inverse square dependence (of the trap amplitude, for a given  $x$ ) on time of Eq. (15), as well as the one the regular harmonic trap of constant amplitude. In both of these cases, as well as more generally, the lens transformation suggests the equivalence with a NLS equation with a gain. In these special cases of interest, the gain is constant or time periodic, suggesting that similar phenomenology to the one of the

regular NLS may be present. A note of caution worth making here is that in reality in this case, the evolution takes place in the setting of Eq. (1), rather than that of Eq. (13). The motivation, however, is that upon suitable choice of the initial condition (and for the types of traps discussed above), the two equations (the GP and the NLS with the gain term) are *equivalent at initial times*, hence one may expect that the instability that is present in the latter will manifest itself in some manner in the former.

However, to examine the details of the time evolution of this instability, we perform numerical simulations of the Eq. (1) with appropriately chosen modulationally stable as well as modulationally unstable initial conditions.

#### IV. NUMERICAL MANIFESTATIONS OF THE MODULATIONAL INSTABILITY FOR NLS WITH QUADRATIC POTENTIAL

##### A. Time-dependent potential

Perhaps the most interesting case (due to the suggested analogy with an NLS with a constant coefficient gain, where

the modulational stability analysis can be performed) is the case of  $k(t) = (t + t^*)^{-2}/16$ , which we now examine numerically.

Notice that in our numerical investigations, we will apply a loss term to Eq. (1) close to the boundaries to emulate the loss of particles from the trap.

The first case that we studied in this setting was the one of an initial condition

$$u(x,t) = \exp\left(i \frac{x^2}{8t^*}\right) [1 + \epsilon \cos(Qx)], \quad (22)$$

suggested by Eqs. (8) and (15)–(17).  $\epsilon$  was typically chosen in the range 0.01–0.1 without significant variation in the qualitative nature of the results. The parameter  $t^*$  was set to 1. The results are shown in Fig. 2, for the case of  $Q = 1$  (left panels) and  $Q = 2$  (right panels).

It is clear from the time evolution shown in the figure that in this setting we obtain (and that is one of the main findings of this work) a *soliton wave train*, formed as a result of the instability, starting from such a modulated plane-wave initial condition. An interesting feature of the obtained soliton train is that emerging solitons are of approximately equal shapes (amplitudes) in the presence of a broadening parabolic potential; in the case when the latter is static, created solitons have essentially different shapes depending on their positions in space, see, e.g., Fig. 4.

One can argue that this outcome may not be a result of the modulational instability given that both modulationally stable and unstable  $Q$ 's lead to such a manifestation. However, a careful inspection of the details of the evolution (see also the short-time runs reported below) outrules that possibility. In particular, the two features that happen for modulationally unstable wave numbers are the following.

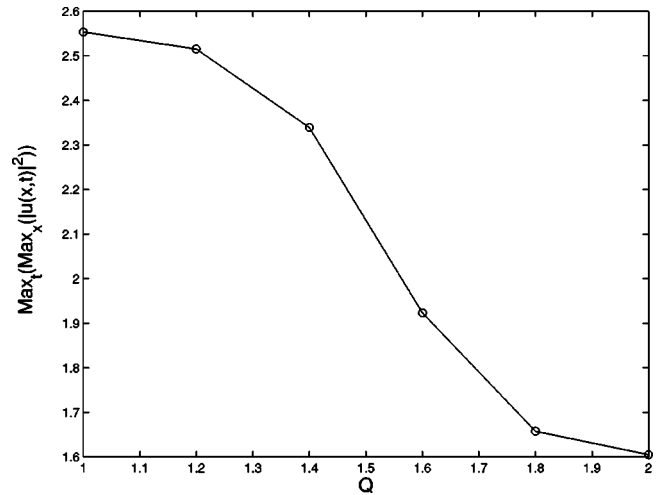


FIG. 3. The maximal amplitude (over space and time) for runs up to  $t = 40$  is shown for different values of the wave number  $Q$  of the perturbation.

(a) The instability is manifested at *earlier times* (see, in particular, the comparison of the third panels of Fig. 2).

(b) The instability leads to *larger amplitudes* in the modulationally unstable regime (see, e.g., the comparison of the fourth panels of Fig. 2), than in the modulationally stable one. This is also clearly shown in Fig. 3, where the cases with different  $Q$  in the perturbation have been examined (for amplitude of the original plane wave  $\phi = 1$ ), showing a clearly larger amplitude tendency for “unstable wave numbers” of  $Q < \sqrt{2}$  in this case.

The reason why in practice the instability occurs in both cases is that the dynamics of the potential in Eq. (1) mix the wave numbers of the original perturbation and eventually

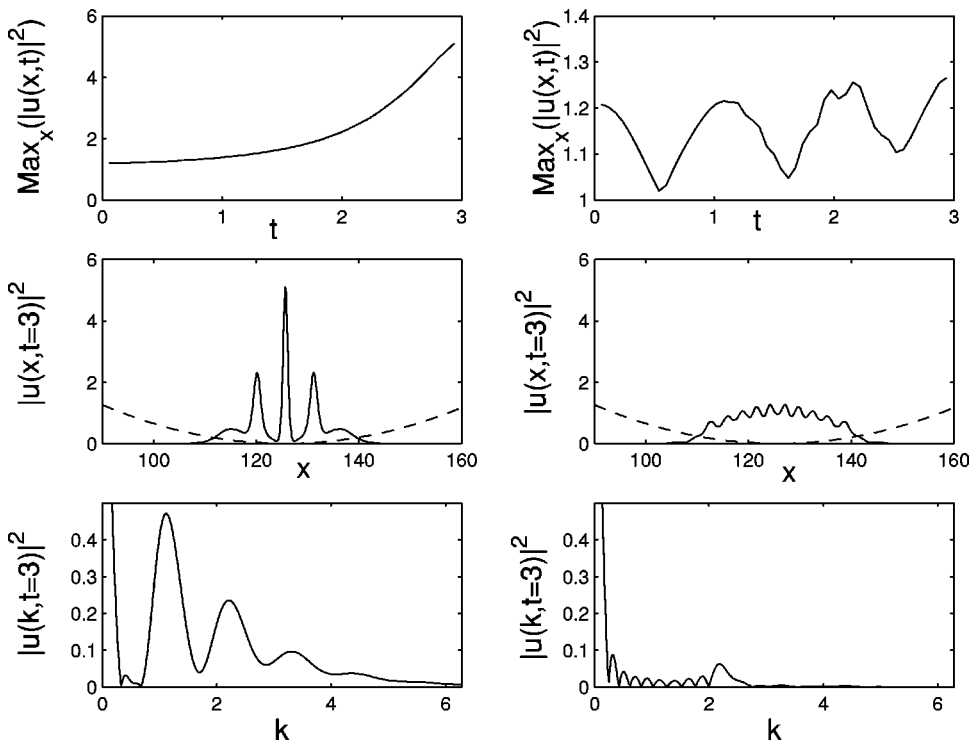


FIG. 4. The cases of  $Q = 1$  (left panels) and  $Q = 2$  (right panels) are shown for the initial condition of Eq. (23). The top panel shows the evolution of the maximum amplitude as a function of time (for short times), the middle panel shows the mod squared spatial profile for  $t = 3$  (the dashed line here illustrates the trap at this time), while the bottom panel shows Fourier transform for the same time ( $t = 3$ ).  $t^* = 5$  has been used here.

result in the excitation of modulationally unstable ones. However, this only happens later (because first the modulationally unstable  $Q$ 's need to be excited) and with a smaller amplitude in this case.

We also tried a different initial condition motivated by the experimental settings that led to the observation of bright matter-wave solitons [7]. In particular, in these settings, a Feshbach resonance is used to tune the sign of the nonlinearity [in the case of Eq. (1) the sign of  $s$ ], starting from the repulsive case of  $s < 0$  and getting to the attractive case of  $s > 0$ , as time evolves in the experiment. Given that in the case of  $s < 0$ , the ground state of the system consists (approximately) of the so-called Thomas-Fermi (TF) cloud [1], we initialized the system in such a state, emulating the time (in the duration of the experiment) in which the system is at  $s < 0$  and evolved the system from such an initial condition. In this case,  $u(x, t=0)$  is of the form

$$u(x, t=0) = u_{TF} [1 + \epsilon \cos(Qx)]. \quad (23)$$

$u_{TF} = \sqrt{\max_x(0, \mu - V(x, t=0))}$  [1]. The chemical potential  $\mu$  is chosen as  $\mu = 1$  in this case.

A particular example of this type for  $\epsilon = 0.1$ ,  $Q = 1$  (left panels), and  $Q = 2$  (right panels) is shown in Fig. 4.

In this case, we only show short-time dynamics, because at longer times the Thomas-Fermi (which is not functionally close to the ground state of the case with  $s = 1$ ) will be destroyed, leading to large amplitude localized excitations independent of the initial value of  $Q$ . In fact, this short time experiment illustrates all the points that we made about (modulationally stable and unstable) short-time evolution previously. The modulationally unstable case of  $Q = 1$  rapidly develops the instability and deforms into a solitary wave train pattern. On the contrary, for the short-times reported in Fig. 4, the modulationally stable case is limited to benign oscillations of small amplitude. In the case of  $Q = 1$ , the sidebands clearly form, indicating the manifestation of the MI. However, notice also, as highlighted previously, that in the case of  $Q = 2$ , the dynamics of Eq. (1) eventually tends to excite modulationally unstable wave numbers and hence will also result (for longer times) in localization.

### B. Time-independent potential

In the case in which the potential is time independent, we first (once again) tried an initial condition with a modulation added to the plane wave in the form

$$u = 1 + \epsilon \cos(Qx). \quad (24)$$

Notice that in this case the chirp was not used in the initial condition as it does not rid the equation of the explicit temporal dependence.

In this case the findings, once again for  $Q = 1$  and  $Q = 2$ , are shown in Fig. 5.  $\epsilon = 0.05$  was used in Eq. (24);  $k = 0.0001$ .

In both cases, for the GP equation, due to the presence of the potential, the condensate will become peaked towards the center, gradually as time evolves. However, the development

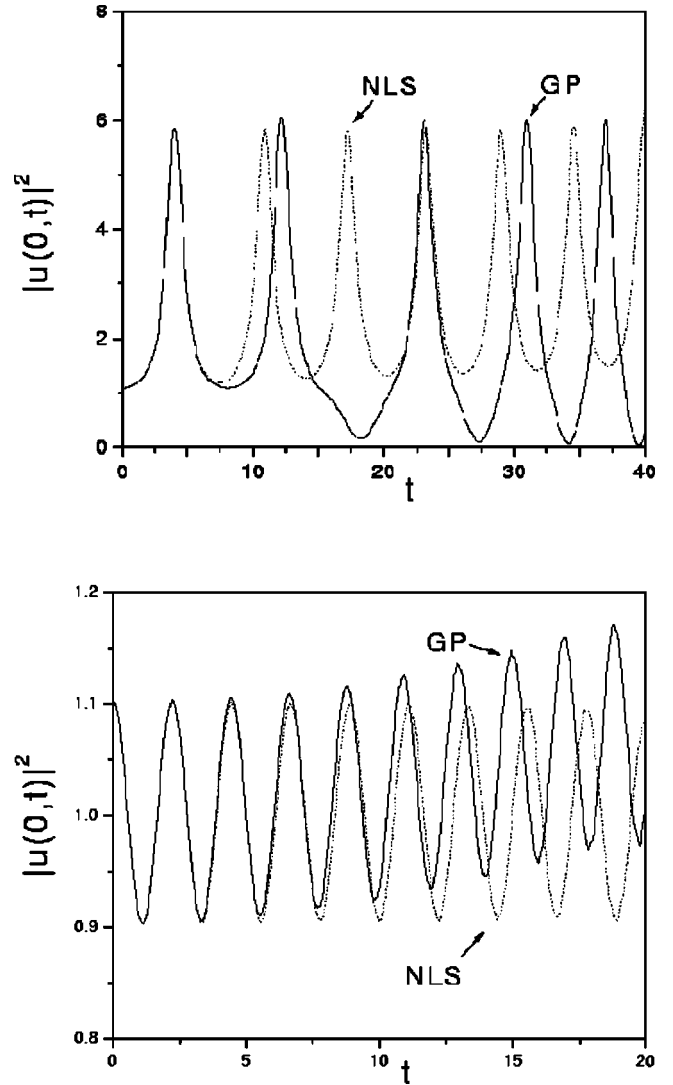


FIG. 5. The time evolution of the amplitude at  $x=0$  ( $|u(0,t)|^2$ ) is shown in the left panel for  $Q=1$  and in the right one for  $Q=2$ . The comparison of the GP Equation (solid line) with the corresponding case for the NLS (dotted line) is also illustrated.

of the instability is clear from the comparison of the corresponding amplitudes of the oscillation of the norm field as a function of time.

The case with the Thomas-Fermi initial condition of Eq. (23) is shown in Fig. 6.  $k = 0.0025$  in this case and once again the cases of  $Q = 1$  and  $Q = 2$  are shown in the left and right panels, respectively.

The development of the instability for short times is once again clear for the modulationally unstable case of  $Q = 1$ , leading to the formation of a wave train, while in the modulationally stable case, the perturbation is not amplified. For longer times, the destruction of the TF cloud will eventually lead in both cases to the generation of very strongly localized patterns. However, in essence here, we take advantage of the separation of time scales for the appearance of the MI and for the destruction of the TF, to illustrate in the short-time evolution, the development of the former instability.

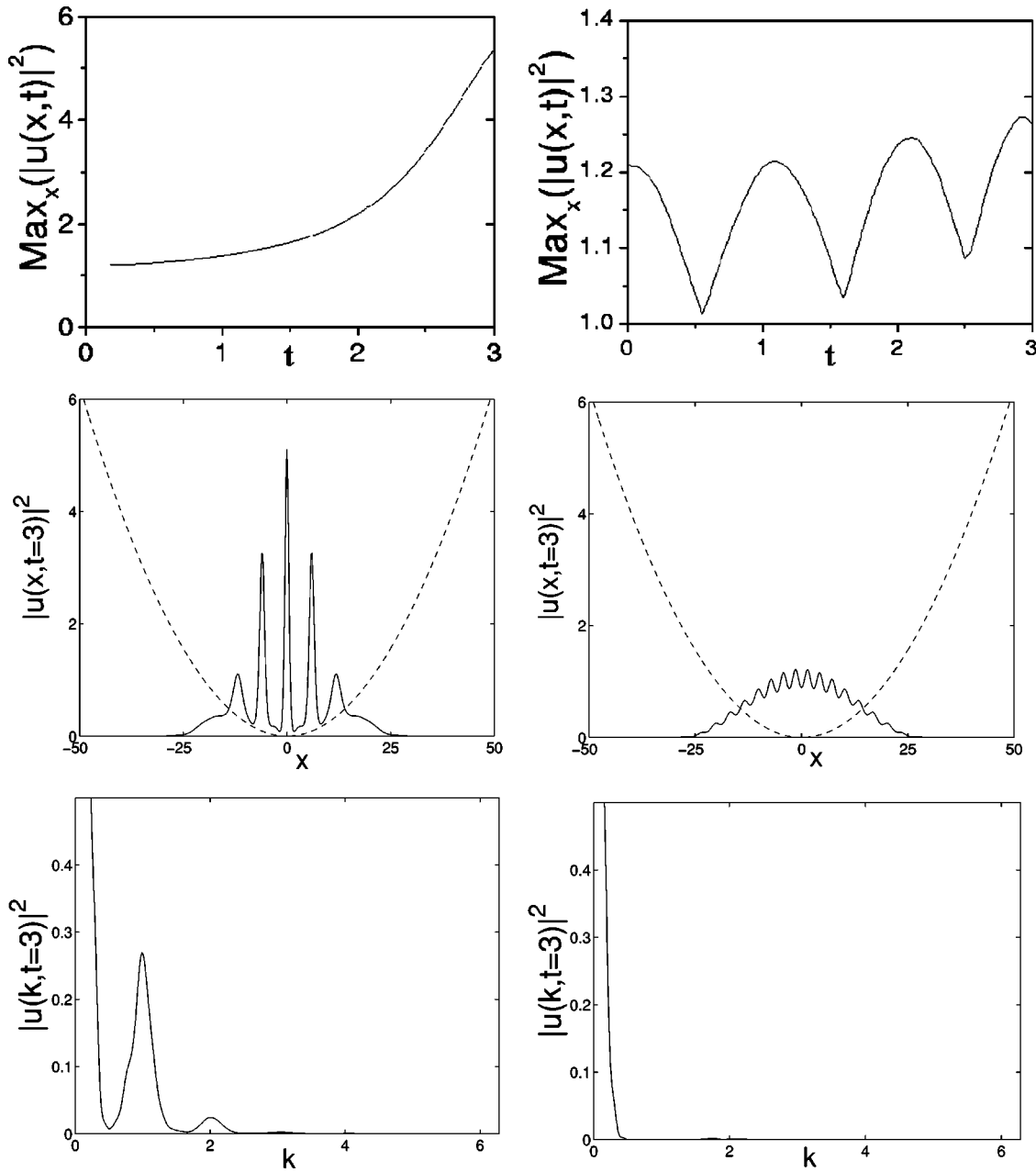


FIG. 6. Same as Fig. 4, but for the case of  $k(t)=0.0025=\text{const}$ . The left panels correspond to  $Q=1$  and the right ones to  $Q=2$ .

V. CONCLUSIONS

In this work, we have examined the problem of modulational instabilities of plane waves in the context of Gross-Pitaevskii equations with an external (in particular, quadratic) potential. The motivation for this study was its direct link to current experimental realizations of Bose-Einstein condensates.

A lens transformation was used to cast the problem in a rescaled space and time frame (in a way very reminiscent of the scaling in problems related to focusing [8,17]). In this rescaled frame, the external potential can be viewed as a form of external growth. For specific forms of temporal dependence of the prefactor of the harmonic potential [e.g., for  $k(t)=(t+t^*)^{-2}/16$ ], the resulting growth term is constant.

In such a context once again the MI analysis can be carried through completely, producing similar conditions, but now in the dynamically rescaled frame/variables (which can be appropriately recast in the original variables). This singles out the case of a temporally dependent potential of inverse square dependence with time. Another case which was also examined due to its direct relevance to the experiment was the one of the constant amplitude trap.

Both of these cases were analyzed theoretically and then studied in detail numerically. The theoretical predictions for modulational instability were verified by the numerical experiments. This was most clearly identified for short-time dynamical evolution results that permit to clearly identify the instability through the formation of localized pulses and trains thereof. For longer times, trains are also formed for

modulationally stable cases (due to the eventual excitation in the dynamics of unstable wave numbers). However, there are still “stronger” signatures of the instability in the unstable cases (such as the larger amplitude of the resulting excitations in such cases).

The main aim of this work is to advocate the use of the MI as an experimental tool to generate solitonic trains in Bose-Einstein condensates. Our theoretical investigation and numerical findings clearly support the formation of such trains in the context of the GP equation initialized with an appropriate modulation and possibly a chirp. The latter is needed in the case of the time-dependent trap that we have examined herein and which we argue may also be interesting to try to create in experimental settings. Let us note in passing that traps with this type of time dependence of their amplitude have also been suggested as being of interest in quite different setups such as the study of explosion-implosion dualities for the quintic (critical) GP [18]. However, our findings should be observable *even without* the

time-dependent trap, as we have demonstrated. The appropriate modulation in the condensate initial condition can be generated by placing the condensate in an optical lattice [19], while the chirp can also be produced using appropriate phase-engineering techniques that are currently experimentally available; see, e.g., Ref. [5]. We believe that such experiments are within the realm of present experimental capabilities and hope that these theoretical findings may motivate their realization in the near future.

#### ACKNOWLEDGMENTS

P.G.K. gratefully acknowledges support from a University of Massachusetts Faculty Research Grant, from the Clay Mathematics Institute, and from the NSF through Grant No. DMS-0204585. V.V.K. gratefully acknowledges support from the European COSYC Grant No. HPRN-CT-2000-00158.

- 
- [1] F. Dalfovo, S. Giorgini, L.P. Pitaevskii, and S. Stringari, *Rev. Mod. Phys.* **71**, 463 (1999); A.J. Leggett, *ibid.* **73**, 307 (2001).
- [2] M.R. Matthews *et al.*, *Phys. Rev. Lett.* **83**, 2498 (1999); K.W. Madison *et al.*, *ibid.* **84**, 806 (2000); S. Inouye *et al.*, **87**, 080402 (2001).
- [3] J.R. Abo-Shaer *et al.*, *Science* **292**, 476 (2001); J.R. Abo-Shaer, C. Raman, and W. Ketterle, *Phys. Rev. Lett.* **88**, 070409 (2002); P. Engels *et al.*, *ibid.* **89**, 100403 (2002).
- [4] S. Burger *et al.*, *Phys. Rev. Lett.* **83**, 5198 (1999).
- [5] J. Denschlag *et al.*, *Science* **287**, 97 (2000).
- [6] B.P. Anderson *et al.*, *Phys. Rev. Lett.* **86**, 2926 (2001).
- [7] K.E. Strecker *et al.*, *Nature (London)* **417**, 150 (2002); L. Khaykovich *et al.*, *Science* **296**, 1290 (2002).
- [8] C. Sulem and P. L. Sulem, *The Nonlinear Schrödinger Equation* (Springer-Verlag, New York, 1999).
- [9] T.B. Benjamin and J.E. Feir, *J. Fluid Mech.* **27**, 417 (1967).
- [10] L.A. Ostrovskii, *Sov. Phys. JETP* **24**, 797 (1969).
- [11] T. Taniuti and H. Washimi, *Phys. Rev. Lett.* **21**, 209 (1968); A. Hasegawa, *ibid.* **24**, 1165 (1970).
- [12] V.V. Konotop and M. Salerno, *Phys. Rev. A* **65**, 021602(R) (2002).
- [13] A. Smerzi, A. Trombettoni, P.G. Kevrekidis, and A.R. Bishop, *Phys. Rev. Lett.* **89**, 170402 (2002).
- [14] F.S. Cataliotti *et al.*, e-print cond-mat/0207139.
- [15] M. Kasevich and A. Tuchman (private communication).
- [16] A. Hasegawa and W.F. Brinkman, *IEEE J. Quantum Electron.* **16**, 694 (1980); K. Tai, A. Tomita, and A. Hasegawa, *Phys. Rev. Lett.* **56**, 135 (1986).
- [17] See, e.g., C.I. Siettos, I.G. Kevrekidis, and P.G. Kevrekidis, *Nonlinearity* **16**, 497 (2003), and references therein.
- [18] P.K. Ghosh, e-print cond-mat/0109073.
- [19] See, e.g., F.S. Cataliotti, S. Burger, C. Fort, P. Maddaloni, F. Minardi, A. Trombettoni, A. Smerzi, and M. Inguscio, *Science* **293**, 843 (2001); M. Greiner, O. Mandel, T. Esslinger, T.W. Hänsch, and I. Bloch, *Nature (London)* **415**, 39 (2002).